

Region-Level Context-Aware Multimodal Understanding

Hongliang Wei, Xianqi Zhang, Xingtao Wang, Xiaopeng Fan, *Senior Member, IEEE*, Debin Zhao, *Member, IEEE*,

Abstract—Despite significant progress, existing research on Multimodal Large Language Models (MLLMs) mainly focuses on general visual understanding, overlooking the ability to integrate textual context associated with objects for a more context-aware multimodal understanding — an ability we refer to as Region-level Context-aware Multimodal Understanding (RCMU). To address this limitation, we first formulate the RCMU task, which requires models to respond to user instructions by integrating both image content and textual information of regions or objects. To equip MLLMs with RCMU capabilities, we propose Region-level Context-aware Visual Instruction Tuning (RCVIT), which incorporates object information into the model input and enables the model to utilize bounding box coordinates to effectively associate objects’ visual content with their textual information. To address the lack of datasets, we introduce the RCMU dataset, a large-scale visual instruction tuning dataset that covers multiple RCMU tasks. We also propose RC&P-Bench, a comprehensive benchmark that can evaluate the performance of MLLMs in RCMU and multimodal personalized understanding tasks. Additionally, we propose a reference-free evaluation metric to perform a comprehensive and fine-grained evaluation of the region-level context-aware image descriptions. By performing RCVIT on Qwen2-VL models with the RCMU dataset, we developed RC-Qwen2-VL models. Experimental results indicate that RC-Qwen2-VL models not only achieve outstanding performance on multiple RCMU tasks but also demonstrate successful applications in multimodal RAG and personalized conversation. Our data, model and benchmark are available at <https://github.com/hongliang-wei/RC-MLLM>

Index Terms—Article submission, IEEE, IEEEtran, journal, L^AT_EX, paper, template, typesetting.

I. INTRODUCTION

MULTIMODAL large language models (MLLMs) [1]–[6] expands language models into the multimodal domain by integrating visual encoders, demonstrating outstanding performance across a range of multimodal tasks, such as visual question answering, document understanding, robotic manipulation, among others.

However, existing MLLMs primarily focus on general visual understanding, lacking the ability to integrate textual context for a more context-aware multimodal understanding. To address this limitation, existing approaches [7]–[9] integrate image-related information into the model’s context

Hongliang Wei, Xianqi Zhang, Debin Zhao are with the Faculty of Computing, Harbin Institute of Technology, Harbin 150001, China.

Xingtao Wang is with the Department of Computer Science and Technology, Harbin Institute of Technology, Harbin 150001, China, and also with Harbin Institute of Technology Suzhou Research Institute, Suzhou 215104, China.

Xiaopeng Fan is with the Department of Computer Science and Technology, Harbin Institute of Technology, Harbin 150001, China, Harbin Institute of Technology Suzhou Research Institute, Suzhou 215104, China and also with the Peng Cheng Laboratory, Shenzhen, China.

Email: hlwei@stu.hit.edu.cn; zhangxianqi@stu.hit.edu.cn; xtwang@hit.edu.cn; fxp@hit.edu.cn; dbzhao@hit.edu.cn

Corresponding author: Xingtao Wang.

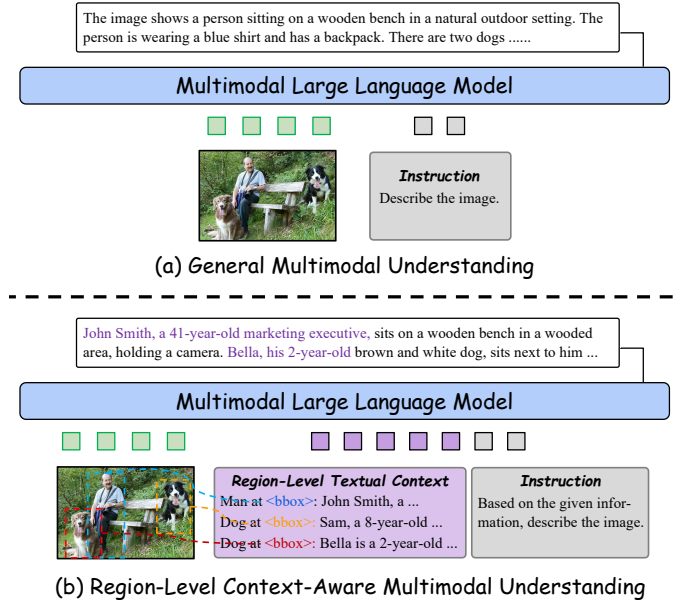


Fig. 1: Illustration of the RCMU Task. RCMU requires MLLMs to respond based on both image content and region-level textual contexts.

window and train the model to leverage this information, achieving image-level context awareness.

In this paper, we push the boundaries of MLLMs even further by endowing them with region-level context awareness, which is a crucial capability for tasks that require fine-grained contextual understanding, such as multimodal personalized conversation and multimodal RAG in complex scenarios. Region-level context-aware multimodal understanding (RCMU) in MLLMs remains an unexplored domain. To bridge this gap, we first formulate the RCMU task, where MLLMs are required to respond to user instructions based on both visual content and textual information of objects, as illustrated in Figure 1.

To equip MLLMs with RCMU capability, we propose Region-level Context-aware Visual Instruction Tuning (RCVIT). During training, RCVIT integrates contextual information about objects into the model input and enables the model to utilize the bounding box coordinates of objects to effectively link the visual content of objects with their textual information. After training, the model can provide region-level context-aware responses for unseen instances without additional fine-tuning.

One significant challenge in advancing RCMU is the lack of large-scale instruction tuning datasets designed specifically for RCMU tasks. To address this challenge, we propose the RCMU dataset, which is designed to enhance the

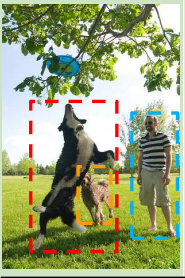
Textual Context:			
	<p>[1]: The information of the man located at $\langle \text{box_start} \rangle(755,417),(991,885)\langle \text{box_end} \rangle$ in the image: John Smith, a 41-year-old marketing executive, resides in downtown Chicago. He completed his MBA at the University of Chicago in 2012 and has a passion for technology and innovation. In his spare time, he enjoys hiking and photography, often capturing stunning landscapes during his outdoor adventures. Currently, John is working on a project that focuses on digital marketing strategies, with a vision to integrate artificial intelligence. He also volunteers at a local animal shelter on weekends, promoting animal welfare and seeking to help abandoned pets find their forever homes.</p> <p>[2]: The information of the dog located at $\langle \text{box_start} \rangle(163,375),(638,936)\langle \text{box_end} \rangle$ in the image: Bella is a 2-year-old dog owned by John Smith, who emphasizes the joy pets bring to daily life. Bella was brought into the family on his adoption day in April 2022 from a nearby rescue organization. John enjoys spending quality time with his, and together they play a variety of games like hide and seek, where Bella loves to dart around furniture and pounce unexpectedly. Bella's preferred activities include watching birds from the window and exploring new boxes or bags that find their way into the house, always keeping John entertained with his curious antics.</p> <p>[3]: The information of the dog located at $\langle \text{box_start} \rangle(442,635),(629,837)\langle \text{box_end} \rangle$ in the image: Sam, a 8-year-old dog, has been a beloved member of the Smith family since his adoption in July 2019. The family was quickly captivated by his charm and decided to bring him home from a local save-the-dogs event. Sam loves to unwind by chasing after his laser toy and sometimes takes it easy by sitting in the family's lap during movie nights. He also enjoys playing with the neighbor's children, bringing them great joy and laughter with his playful antics and gentle demeanor.</p> <p>System Prompt: Answer the following question based on the information above and the given image, and provide citations for your response.</p>		
	RCID & MCGG	RVCQA & MCGG Visual-to-Context QA	RVCQA Unanswerable Visual-to-Context QA
	<p>Describe the image.</p> <p>RC-Qwen2-VL: John Smith, a 34-year-old marketing executive [1], is standing on the grass. Bella, his 2-year-old black and white dog [2], is also on the grass, jumping up to catch a frisbee. Sam, an 8-year-old brown dog [3], is also on the grass. The sky is visible over the grass. ✓</p> <p>Qwen2-VL: In the image, there is a woman standing in a grassy field with two dogs. One dog is a black and white border collie, and the other is a brown poodle. The woman is wearing a striped shirt and beige shorts. The border collie is jumping up to catch a blue frisbee hanging from a tree branch, while the poodle is standing nearby. ✗</p>	<p>What activities does the behind dog in the picture enjoy?</p> <p>RC-Qwen2-VL: The Dog enjoys unwinding, chasing after his laser toy, and sitting in the family's lap during movie nights.[3] ✓</p> <p>Qwen2-VL: The behind dog in the picture, Bella, enjoys playing hide and seek, watching birds from the window, and exploring new boxes or bags that find their way into the house. ✗</p>	<p>What kind of training has the dog behind received?</p> <p>RC-Qwen2-VL: Cannot be answered. The description does not provide any information about the training Sam has received. ✓</p> <p>Qwen2-VL: The dog behind has received training to catch the frisbee. ✗</p>
	RVCQA & MCGG Context-to-Visual QA	RVCQA Unanswerable Context-to-Visual QA	
	<p>What does the dog that enjoys watching birds look like?</p> <p>RC-Qwen2-VL: The dog is a black and white dog.[2] ✓</p> <p>Qwen2-VL: The dog that enjoys watching birds is a 2-year-old dog named Bella. ✗</p>	<p>What color is the dog that had a serious illness this year?</p> <p>RC-Qwen2-VL: There is no information about the dog that had a serious illness this year, so it is not possible to answer this question. ✓</p> <p>Qwen2-VL: There is no dog in the image that had a serious illness this year. ✓</p>	

Fig. 2: Responses of RC-Qwen2-VL 7B and Qwen2-VL 7B on RCMU tasks. RC-Qwen2-VL performs better on RCMU tasks, accurately aligning visual content of objects with their textual context and providing relevant contextual references.

RCMU capability of MLLMs. It encompasses multiple RCMU tasks, such as Region-level Context-aware Image Description (RCID), Region-level Context-aware Visual Question Answering (RVCQA), and Multimodal Contextual Citation Generation (MCCG), all of which require the simultaneous understanding of both visual content and textual context. To develop the RCMU dataset, we introduce an automated data annotation pipeline that uses language models to generate textual context for object instances in referring expression generation (REG) datasets [10]–[13], and cleverly constructs region-level context-aware image descriptions and question-answer pairs. The proposed RCMU dataset comprises 84k images, 102 object categories, 1.3K personalized information, 1M contextualized image descriptions, and 6.9M contextualized-VQA quadruples, advancing region-level multimodal understanding in MLLMs.

Furthermore, we introduce RCIDScore, a novel reference-free evaluation metric for comprehensively evaluating the quality of region-level context-aware image descriptions. Unlike traditional metrics [14]–[17] that provide a single score, RCIDScore evaluates contextualized descriptions from both contextual and visual perspectives, providing a more fine-grained assessment. Particularly in terms of contextual perspective, it offers a detailed evaluation by measuring the coverage and accuracy of contextual information within the description, as well as the region-level consistency between the contextual and visual information.

Finally, to promote the development of Region-Level Context-Aware Multimodal Understanding and its application in multimodal personalized understanding, we propose RC&P-Bench. It evaluates a model's fine-grained and personalized multimodal understanding of specific entities in the image. This is achieved by providing multi-view, multi-scenario visual reference images of entities, along with their complex personalized information, and requiring the model to perform

visual question answering based on this multimodal data. This makes RC&P-Bench a comprehensive evaluation platform.

II. RELATED WORK

A. Multimodal Large Language Models (MLLMs)

MLLMs use bridging layers to connect vision encoders with language models, achieving strong performance in multimodal understanding and generation tasks. In terms of bridging mechanisms, Flamingo [2] introduced a gated cross-attention layer to align multimodal features without fine-tuning encoders. BLIP-2 [18] and InstructBLIP [5] used Q-Former to transform visual inputs into language-like queries for better text alignment. The LLaVA [19] series used linear projections to align visual features with frozen language models. Recent studies [6], [20] highlight the use of multiple vision encoders to handle diverse visual tasks and improve feature representation. High-resolution inputs enhance visual understanding and task performance [4], [21], [22]. Multimodal in-context learning [2], [23] and chain-of-thought reasoning [24], [25] have been explored to enhance performance. MLLMs have also been extended to video [26]–[28], 3D data [29], [30], and embodied intelligence [31], [32].

B. Context-Aware Multimodal Understanding in MLLMs

Context-aware multimodal understanding is a crucial capability of MLLMs. By utilizing context window, MLLMs can understand information in specific scenarios and generate coherent, relevant responses. For example, MMICL [8] leverages multimodal in-context learning to enhance MLLMs' understanding of complex prompts, improving their zero-shot performance in various vision-language tasks. MuRAG [7] integrates image and text information using an external multimodal memory to enhance the accuracy of open-domain VQA. CaMML [9] uses relevant multimodal examples

during inference to enhance the understanding and generation abilities of MLLMs.

Unlike these works that primarily focus on image-level context awareness in MLLMs, this work takes a step further by equipping MLLMs with region-level context awareness, a direction that remains unexplored.

C. Multimodal Personalized Understanding

Personalized multimodal understanding, which aims to enable user-specific multimodal understanding, is a topic closely related to region-level context-aware multimodal understanding. RAP-MLLM [33] uses a retrieval-augmented framework with a key-value database to flexibly incorporate and update personalized concepts in real time. Yo’LLaVA [34] introduces learnable tokens representing user-specific objects from a few images, efficiently adapting the model with minimal training and hard negative samples to improve recognition. MyVLM [35] employs external concept heads to add personalized embeddings learned from limited user data, enhancing vision-language tasks while keeping the base model unchanged. Compared to these models, our model can achieve more complex multimodal personalized understanding with a retrieval mechanism.

III. METHOD

This section provides a detailed exposition of the RCMU task formulation (Section III-A), the RCMU dataset (Section III-B), the RCVIT approach III-C), and the RCIDScore metric (Section III-D).

A. RCMU Task Formulation

In the RCMU task, the model is required to respond to user instructions based on both the visual content and the textual context of objects. In this work, the textual context of objects includes the bounding box coordinates of the objects in the image as well as their personalized information.

Formally, let P be an image, I be an instruction, and $C = \{c_1, c_2, \dots, c_k\}$ denote the textual information of objects, where k represents the number of objects with textual information. The MLLM is then tasked with generating a region-level context-aware response R :

$$R = \text{MLLM}(P, C, I) \quad (1)$$

B. RCMU Dataset and Construction Pipeline

The RCMU dataset covers three region-level context-aware multimodal understanding tasks: 1) **Region-level Context-aware Image Description (RCID)**: the model needs to provide a contextualized image description based on the image and the contextual information of the objects. 2) **Region-level Context-aware Visual Question Answering (RCVQA)** for both answerable and unanswerable questions: the model needs to answer contextual questions based on visual references or answer visual questions based on contextual references. The questions include both answerable and unanswerable ones. 3) **Multimodal Contextual Citation Generation (MCCG)**: the

model is required to generate responses that include citations referencing the relevant context. All of these tasks require the simultaneous understanding of visual content and textual context. The statistical information of the RCMU dataset is presented in Table I.

We developed an automated data annotation pipeline to generate high-quality annotations for the RCMU dataset. Built on existing Referring Expression Generation (REG) datasets [10]–[13], our pipeline first employs LLMs¹ to generate personalized information (i.e., textual context) for objects in images. It then utilizes object bounding boxes, visual referring expressions, and grounded image descriptions from REG datasets, combined with the generated personalized information, to construct diverse tasks that require a simultaneous understanding of visual content and personalized information for accurate completion. As illustrated in Figure 5, the framework operates in three main stages:

- **Textual Context Generation.** We prompt GPT-4o to generate multiple unique personalized information for each object category, which are then assigned to objects in the image based on their categories. To avoid any conflicts between the generated information and the visual content in the image, GPT-4o is explicitly instructed to avoid generating any visual information about the objects.
- **RCVQA Construction.** In this stage, we construct QA pairs that require an integrated understanding of both visual content and textual context. This is achieved by referencing objects using details from one modality and posing questions about the other modality. For example, we may describe an object with textual context information and ask the model about its visual characteristics, or vice versa. Additionally, to ensure the model genuinely comprehends the textual context, we create two types of challenging unanswerable questions. One type asks about details not mentioned in the textual context, while the other type inquires about the visual attributes of objects that do not exist in the image. Specifically, 1) the pipeline begins by using an LLM to extract structured information separately from visual referring expressions and textual context. This structured information is then utilized to generate visual QA pairs, contextual QA pairs, contextual referring expressions, and unanswerable contextual QA pairs. To further enhance data quality, the generated referring expressions and QA pairs undergo a meticulously designed filtering process. For QA pairs, LLMs are utilized to assess their validity and informativeness, with higher-scoring pairs being selected. For referring expressions, a text similarity model is used to filter and retain only unique expressions, ensuring that each referring expression unambiguously refers to a single object. 2) During the pronoun substitution step, pronouns referring to objects in contextual questions are replaced with visual referring expressions, resulting in image-to-context VQA pairs. Conversely, in visual questions, pronouns are substituted with contextual referring expressions to generate context-to-image VQA pairs. To construct unan-

¹All prompts used in the pipeline are displayed in the appendix.

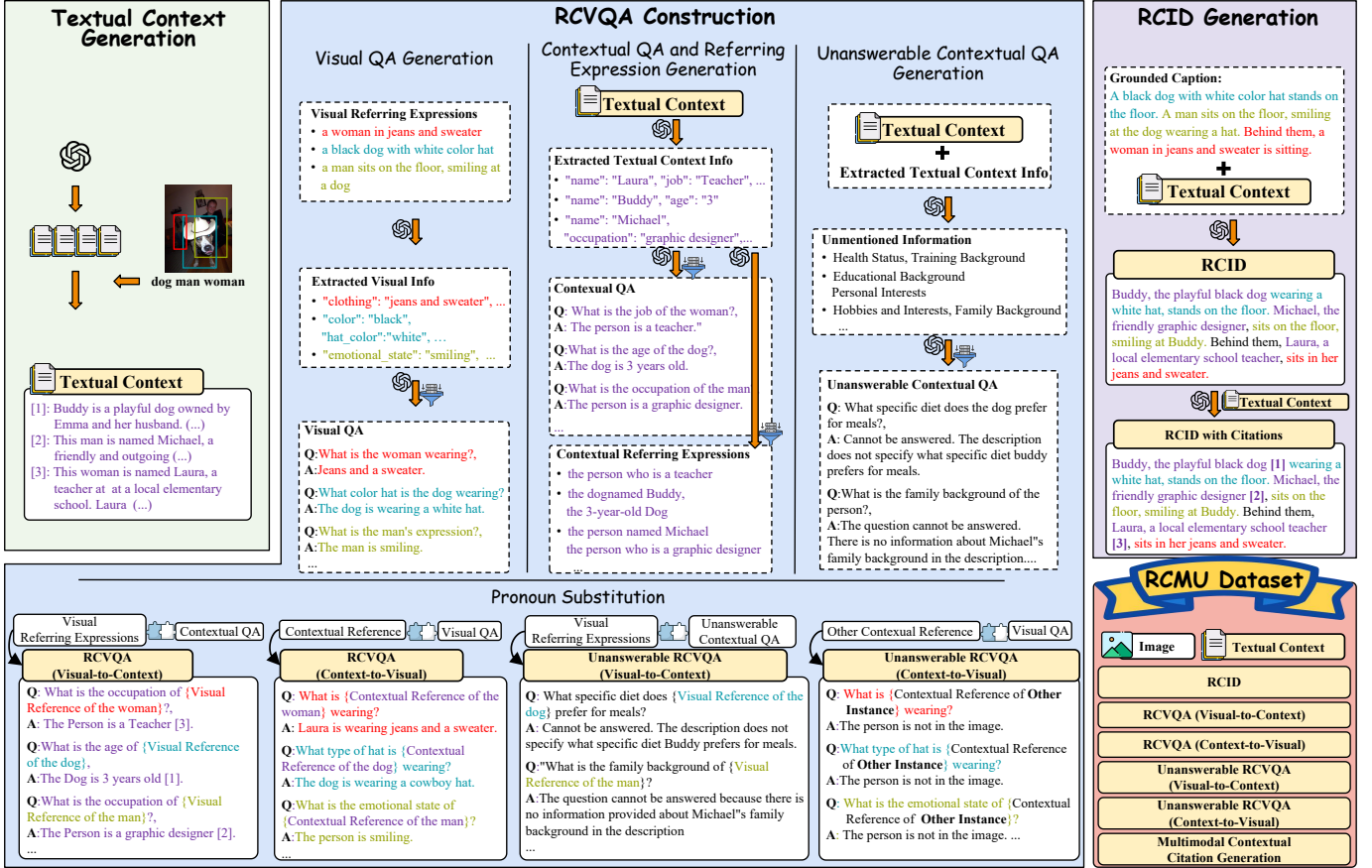


Fig. 3: Automatic data construction pipeline for the RCMU dataset. This pipeline can generate high-quality training data for multiple RCMU tasks, including answerable/unanswerable RCVQA, RCID and MCGG.

swerable image-to-context VQA pairs, the framework replaces object-referring pronouns in unanswerable contextual questions with visual referring expressions. For unanswerable context-to-image VQA pairs, pronouns are replaced with contextual referring expressions of objects that do not exist in the image.

- **RCID Generation.** We adopt a two-step approach to generate region-level context-aware image descriptions with citations. In the first step, GPT-4o is prompted to create a contextualized image description by integrating grounded image descriptions with relevant textual context. Then, GPT-4o further refines the description by incorporating citations about relevant contextual information.

Finally, we obtain the RCMU dataset, comprising 84,149 images, 102 object categories, and 1,352 object instances with contextual information. The dataset includes 1,027,681 contextualized image descriptions and 6,954,726 unique RCVQA quadruples, providing a comprehensive and diverse resource for advancing RCMU in MLLMs.

We also manually annotated an RCMU test set specifically for evaluating RCID, RCVQA, and MCGG tasks. Specifically, we randomly selected 118 images from the Refcog dataset, ensuring a balanced mix of images containing different numbers of objects. We provided textual context for each annotated object in these images. Then, we annotated region-level context-aware image descriptions and region-level context-

RCMU dataset statistics:

Number of images	84,149
Number of object categories	102
Number of personalized information	1,352
Number of contextualized image descriptions	1,027,681
Number of unique RCVQA quadruples	6,954,726
↔ Context-to-image quadruples with answerable question	2,168,408
↔ Image-to-context quadruples with answerable question	1,670,746
↔ Context-to-image quadruples with unanswerable question	2,524,128
↔ Image-to-context quadruples with unanswerable question	591,444
Average number of objects per image	2.29
Average context length per instance (words)	50.91
Average contextualized image descriptions length (words)	55.69
Average number of citations per description	55.69
Average question length (words)	12.13
Average answer length (words)	13.75

TABLE I: **RCMU dataset Statistics.** RCMU dataset is the first large-scale region-level context-aware visual instruction tuning dataset.

aware VQA pairs for these images. These VQA pairs, totaling 6,637, encompass two types—visual-to-context and context-to-visual—and include both answerable and unanswerable questions. Notably, the images and object information in the test set are entirely distinct from those in the training set.

C. RCVIT

The RCVIT incorporates the textual context of objects into the model input, formatted as: 'The

<object> located at <[x1, y1, x2, y2]> in the image:<object information>\n<instruction>. During training, RCVIT trains MLLMs to leverage the bounding box coordinates to associate and fuse the visual and textual information of objects. After training, MLLMs can generate region-level context-aware responses for unseen instances without additional fine-tuning.

Technically, we represent training dataset as $\mathcal{D} = \{I^i, C^i, Q^i, R^i\}_{i=1}^N$, where I^i , Q^i , and R^i represent the image, user query, and model response, respectively. $C^i = \{c_1^i, c_2^i, \dots, c_k^i\}$ denotes the textual context with object bounding boxes, k denotes the number of objects with textual information in the image. And the optimization problem can be formalized as:

$$\mathcal{L}(\mathcal{D}) = -\frac{1}{N} \sum_{i=1}^N \log p(R_i | \mathcal{F}(I^i, C^i, Q^i)) \quad (2)$$

After performing RCVIT on Qwen2-VL models using the RCMU dataset, we developed RC-Qwen2-VL models, which demonstrate powerful RCMU capabilities.

D. RCIDScore

RCIDScore is a reference-free evaluation metric that assesses region-level context-aware image descriptions from both contextual and visual aspects, offering a more fine-grained evaluation, as illustrated in Figure 4.

The RCIDScore evaluates contextual aspects from three key perspectives: contextual coverage, contextual accuracy, and region-level context-visual consistency.

- **Contextual Coverage.** Contextual coverage measures the proportion of objects whose contextual information is mentioned (denoted as RCIDScore_{cc}).

$$\text{RCIDScore}_{cc} = \frac{|\{\text{objects whose context is mentioned}\}|}{|\{\text{all objects with context}\}|} \quad (3)$$

We prompt an LLM² to check if an object’s textual context is mentioned in the image description.

- **Contextual Accuracy.** Contextual accuracy measures the probability that the contextual information of the mentioned objects is entirely correct (denoted as RCIDScore_{ca}):

$$\text{RCIDScore}_{ca} = \begin{cases} 0 & \text{if } N = 0 \\ \frac{|\{\text{objects with correctly mentioned context}\}|}{N} & \text{if } N > 0 \end{cases} \quad (4)$$

where N represents the number of objects whose contextual information is mentioned in the image description. We prompt an MLLM to verify whether the textual context of each object is accurately mentioned.

- **Context-Visual Consistency.** Since the model may make errors when associating the visual content with the textual context of objects, we introduce the region-level context-visual consistency metric to evaluate the alignment between the visual content and textual context of

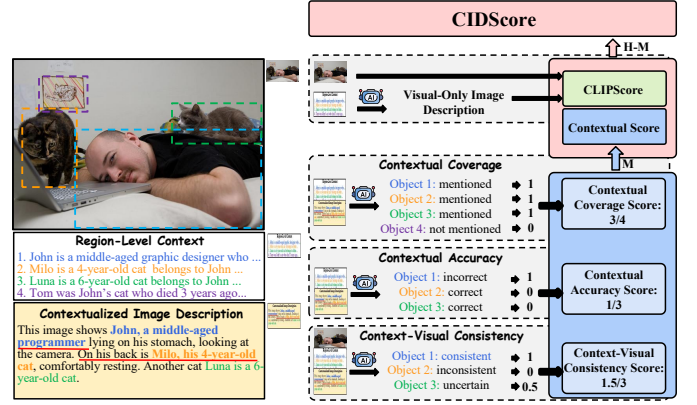


Fig. 4: The RCIDScore evaluates contextualized image descriptions from both visual content and textual context perspectives. For the textual context, it employs a carefully designed evaluation method that considers contextual coverage, contextual accuracy, and region-level context-visual consistency.

objects in the description. Given that the description may include only the textual context of an object without referencing its visual content, we define three possible scores when prompting an MLLM to assess consistency: consistency score $\in \{\text{Consistent} = 1, \text{Inconsistent} = 0, \text{Uncertain} = 0.5\}$. The context-visual consistency metric (denoted as RCIDScore_{cvc}) is calculated as:

$$\text{RCIDScore}_{cvc} = \begin{cases} 0 & \text{if } N = 0 \\ \frac{\sum_{i=1}^N \text{consistency score}_i}{N} & \text{if } N > 0 \end{cases} \quad (5)$$

where N represents the number of objects whose textual context is mentioned in the image description.

By combining these three scores, we propose a comprehensive metric (denoted as RCIDScore_{ctx}) to evaluate the quality of region-level context-aware image descriptions from a contextual perspective:

$$\text{RCIDScore}_{ctx} = \frac{\text{RCIDScore}_{cc} + \text{RCIDScore}_{ca} + \text{RCIDScore}_{cvc}}{3} \quad (6)$$

For the visual perspective, we use CLIPScore [36] to assess the quality of contextualized image descriptions. To obtain a larger text input window, we replace the CLIP model in CLIPScore with the LLM2CLIP [37] model. Since the textual context of objects in the descriptions is not directly linked to the image and may interfere with assessment, we first utilize an LLM to filter out this context before evaluation, ensuring a more accurate assessment.

Finally, we present RCIDScore, a comprehensive evaluation metric that assesses the quality of contextualized image descriptions from both visual and contextual perspectives:

$$\text{RCIDScore} = \text{H-Mean}(\text{RCIDScore}_{ctx}, \text{CLIPScore}) \quad (7)$$

The above metrics collectively provide a more comprehensive and fine-grained evaluation of region-level context-aware image descriptions.

²All prompts used in the RCIDScore are displayed in the appendix.

	<p>This 'Mischievous Rabbit' figurine belongs to Isabella Morgan, a 29-year-old children's book illustrator from Melbourne, Australia. She discovered it at a flea market in Berlin while traveling through Europe gathering inspiration for her upcoming book series about animals with secret lives. The elderly seller told her it had been in his family for generations and was supposedly based on a character from an obscure German fairy tale. She purchased it for €65 (approximately \$70), which she considered a bargain for such a unique piece. Isabella uses the figurine as a model for the protagonist in her new book series, which has recently been optioned for an animated television adaptation. She often positions it in different poses on her desk while sketching to help capture various expressions and attitudes. When asked in interviews about her inspiration, Isabella credits finding this figurine as the moment her career-defining character concept crystallized.</p>				
	<p>This 'White Jade and Copper Jade Rabbit' luxury figurine belongs to Victoria Blackwell, a 63-year-old retired ambassador who served in diplomatic missions across Asia for three decades. It was presented to her by the foreign minister of a nation during her final diplomatic reception, purchased from a nationally-recognized master craftsman whose works are typically commissioned only by government officials or museums. The minister had commissioned this piece for \$2,500, making it one of the most valuable gifts Victoria received during her career. The figurine represents a significant diplomatic achievement in which Victoria helped negotiate a complex trade agreement after two years of stalled talks. Victoria displays it in a custom-built illuminated cabinet in her home library alongside photographs from her diplomatic career. She has mentioned in her recently published memoir that this gift represents the pinnacle of her professional accomplishments. Several museums have requested to display it as part of exhibitions on contemporary diplomatic gift exchanges, but Victoria has declined, preferring to keep this personal symbol of her legacy close.</p>				
	<p>This figurine is owned by Charlotte Zhang, a 52-year-old quantum physics professor at MIT who pioneered a breakthrough in quantum computing architecture. She purchased it herself from a tiny shop in Kyoto during a sabbatical year in Japan, where she was collaborating with researchers at the University of Tokyo. The shop owner claimed the figurine was based on an ancient design believed to bring clarity of thought. Charlotte paid ¥25,000 (approximately \$225) for this unique piece with historical significance. Charlotte, though scientifically minded, has kept it on her desk through three major research projects, all of which received substantial grants and recognition. Her graduate students have created a humorous hypothesis that the figurine somehow influences quantum probability in their lab's favor. Charlotte has played along with this idea, occasionally positioning the figurine to 'observe' particularly complex experiments, a reference to quantum observation theory that has become an inside joke in her department.</p>				
	<p>This figurine belongs to Miguel Fernandez, a 47-year-old former professional soccer player who now coaches an emerging team in Argentina. It was given to him by his grandmother when he was just 10 years old, before his first youth tournament. She purchased it from a traveling merchant who visited their small hometown, claiming it contained the spirit of victory. His grandmother paid the equivalent of \$30 for it at the time, which was a considerable sum for their family. Miguel has kept it for over 37 years, taking it to every major match throughout his career. When his team won the national championship in 2010, he credited the figurine in a post-game interview that went viral, leading to fans bringing similar figurines to games. Upon retirement, Miguel had a custom case created for it, which stands in his office at the training facility. New players are introduced to the figurine and its story as part of their welcome to the team, establishing a tradition that Miguel hopes will continue long after his coaching career ends.</p>				
	<p>V2C Questions</p> <table border="0"> <tbody> <tr> <td data-bbox="495 1039 982 1186"> <p>Who is the owner of the figurine in the red box?</p> <p>A. Charlotte Zhang B. Miguel Fernandez C. Isabella Morgan D. Victoria Blackwell E. There is not enough information to answer the question</p> </td> <td data-bbox="982 1039 1490 1186"> <p>What was the purchase time of the figurine in the blue box?</p> <p>A. At Victoria's retirement B. During sabbatical year C. there is not enough information to answer the question D. 37+ years ago</p> </td> </tr> </tbody> </table> <p>C2V Questions</p> <table border="0"> <tbody> <tr> <td data-bbox="495 1228 982 1381"> <p>Which figurine was purchased over 37 years ago?</p> <p>A. The doll in the yellow box B. The doll in the red box C. The doll in the green box D. The doll in the blue box E. There is not enough information to answer the question</p> </td> <td data-bbox="982 1228 1490 1381"> <p>Which figurine is owned by Victoria Blackwell?</p> <p>A. The doll in the red box B. The doll in the yellow box C. The doll in the blue box D. The doll in the green box E. There is not enough information to answer the question</p> </td> </tr> </tbody> </table>	<p>Who is the owner of the figurine in the red box?</p> <p>A. Charlotte Zhang B. Miguel Fernandez C. Isabella Morgan D. Victoria Blackwell E. There is not enough information to answer the question</p>	<p>What was the purchase time of the figurine in the blue box?</p> <p>A. At Victoria's retirement B. During sabbatical year C. there is not enough information to answer the question D. 37+ years ago</p>	<p>Which figurine was purchased over 37 years ago?</p> <p>A. The doll in the yellow box B. The doll in the red box C. The doll in the green box D. The doll in the blue box E. There is not enough information to answer the question</p>	<p>Which figurine is owned by Victoria Blackwell?</p> <p>A. The doll in the red box B. The doll in the yellow box C. The doll in the blue box D. The doll in the green box E. There is not enough information to answer the question</p>
<p>Who is the owner of the figurine in the red box?</p> <p>A. Charlotte Zhang B. Miguel Fernandez C. Isabella Morgan D. Victoria Blackwell E. There is not enough information to answer the question</p>	<p>What was the purchase time of the figurine in the blue box?</p> <p>A. At Victoria's retirement B. During sabbatical year C. there is not enough information to answer the question D. 37+ years ago</p>				
<p>Which figurine was purchased over 37 years ago?</p> <p>A. The doll in the yellow box B. The doll in the red box C. The doll in the green box D. The doll in the blue box E. There is not enough information to answer the question</p>	<p>Which figurine is owned by Victoria Blackwell?</p> <p>A. The doll in the red box B. The doll in the yellow box C. The doll in the blue box D. The doll in the green box E. There is not enough information to answer the question</p>				

Fig. 5: Illustrative Example from RC&P-Bench

IV. RC&P-BENCH

RC&P-Bench contains 3269 multiple-choice questions, covering 259 entities. Each question image contains at least two personalized entities, and all personalized entities within a single image belong to the same category. The average length of personalized information for each entity is 128.1 words.

To construct RC&P-Bench, we first collected images of the same entity in different scenarios or from various perspectives. For person entities, we used real information. For object entities, we used GPT-4o to generate their personalized information. To create the question images, we used the Gemini 2.0 Flash Preview Image Generation to generate various scene images and employed the FLUX.1-Redux model to replace objects in these scenes with entities. We manually checked

these images to ensure that the entity in the question image is consistent with the appearance of the entity in its reference image. We used an AI-assisted approach to generate the questions and options. First, GPT-4o was used to extract key information from the entities' personalized descriptions. This key information was then combined with the visual information of the entities in the image to formulate the question and the correct answer. Key information from other entities in the image and an option stating "there is not enough information to answer the question" were used as distractor options.

To ensure that solving the questions in RC&P-Bench requires the model to simultaneously understand both the image and the entities' personalized information, we designed the

	RCVQA					RCID					
	V2C	C2V	UA V2C	UA C2V	Overall	CC	CA	CVC	RCIDStx	CLIPS	RCIDS
Proprietary											
Gemini Flash 1.5 8B	58.73	37.64	68.61	25.48	47.61	20.88	26.97	26.77	24.87	87.11	38.70
Gemini Flash 1.5	70.43	42.76	70.88	43.4	56.87	11.75	17.24	18.48	15.82	90.25	26.93
Gemini Flash 2.0	59.49	40.65	76.56	41.15	54.46	17.82	22.22	20.94	20.33	84.76	32.79
GPT-4o-mini	49.60	28.95	56.34	33.15	42.01	44.25	63.18	58.26	55.23	78.00	64.67
Open-source											
InternVL2-2B	51.19	30.4	13.18	1.01	23.94	18.72	29.27	22.86	23.62	83.70	36.84
InternVL2-4B	49.26	32.52	36.44	9.24	31.87	55.03	59.49	56.50	57.01	83.20	67.66
InternVL2-8B	52.85	35.30	39.57	20.97	37.17	52.95	61.41	59.20	57.85	83.71	68.42
MiniCPM V2.6 (8B)	51.90	33.18	15.58	4.51	26.30	40.95	48.43	42.96	44.12	80.67	57.04
Qwen2-VL 2B	25.80	9.47	24.81	4.51	16.15	16.30	26.28	20.58	21.05	55.78	30.57
RC-Qwen2-VL 2B (Ours)	<u>70.95</u> +45.15	<u>50.45</u> +40.98	<u>75.51</u> +50.70	<u>95.83</u> +91.32	<u>73.18</u> +57.03	<u>97.38</u> +81.08	<u>97.09</u> +70.81	<u>81.65</u> +61.07	<u>92.04</u> +70.99	<u>68.67</u> +12.89	<u>78.66</u> +48.09
Qwen2-VL 7B	49.49	34.86	20.67	14.54	29.89	28.89	32.66	27.05	29.53	83.08	43.58
RC-Qwen2-VL 7B (Ours)	80.01 +30.52	59.24 +24.38	85.96 +65.29	97.86 +83.32	80.77 +50.88	97.98 +69.09	95.17 +62.51	85.85 +58.80	93.00 +63.47	73.92 -9.16	82.37 +38.79

TABLE II: Experimental results (%) on region-level context-aware multimodal tasks. V2C and C2V denote region-level visual-to-context VQA and region-level context-to-visual VQA, respectively. UA stands for unanswerable. CC, CA, and CVC represent the contextual coverage score, contextual accuracy score, and context-visual consistency score, respectively. Among open-source models, the best results are highlighted in **bold**, while the second-best results are underlined. RC-Qwen2-VL models not only lead their similarly sized open-source counterparts but also outperform certain closed-source models.

Model	Type	Closed-World			Open-World			Oracle		
		C2V	V2C	Overall	C2V	V2C	Overall	V2C	Overall	
GPT-4o	Proprietary	38.18	45.15	46.75	62.04	66.27	65.18	67.79	78.51	71.29
Gemini Pro 2.5		64.06	64.31	68.56	63.09	59.58	66.23	77.18	77.39	79.23
InternVL2-2B	Open-source	22.30	24.64	28.10	26.99	40.12	36.35	35.12	35.16	39.26
InternVL2-4B		20.66	19.68	27.09	53.84	48.38	52.45	47.35	34.41	45.06
InternVL2-8B		26.10	32.61	<u>31.81</u>	<u>57.05</u>	<u>50.04</u>	<u>51.66</u>	<u>75.69</u>	<u>72.35</u>	<u>65.61</u>
MiniCPM V2.6 (8B)		22.60	26.00	30.67	40.87	45.15	46.01	57.05	52.97	53.80
RAP-LLaVA 13B		4.77	5.11	4.97	6.26	6.46	6.13	7.31	7.21	7.27
Qwen2-VL 2B		24.01	31.03	25.18	14.84	32.91	22.18	41.61	53.34	39.66
RC-Qwen2-VL 2B (Ours)	<u>29.38</u> +5.37	<u>34.49</u> +3.46	<u>30.43</u> +5.25	<u>54.74</u> +39.90	<u>46.13</u> +13.22	<u>45.61</u> +23.43	<u>62.12</u> +20.51	<u>62.89</u> +9.55	<u>52.76</u> +13.10	
Qwen2-VL 7B	25.35	30.73	31.26	32.29	44.55	39.75	59.88	62.58	56.90	
RC-Qwen2-VL 7B (Ours)	43.70 +18.35	43.65 +12.92	42.45 +11.19	70.54 +38.25	53.94 +9.39	57.70 +17.95	93.81 +33.93	88.58 +26.00	78.83 +21.93	

TABLE III: Experimental results (%) on RC&P-Bench. V2C and C2V denote Visual-to-Context VQA and Context-to-visual VQA. The best result in each setting is bold and the second is underlined in the open-source models.

Method	Train	#Image	Visual	Text-only	Weighted
MyVLM-LLaVA (13B)	✓	5	91.18	-	-
YoLLaVA (13B)	✓	5	92.94	<u>88.25</u>	90.60
RAP-LLaVA (13B)	✗	1	93.53	93.75	93.64
RAP-Phi3-V (3.8B)	✗	1	94.12	85.00	89.56
Qwen2-VL 2B	✗	0	95.29	85.00	90.15
RC-Qwen2-VL 2B (Ours)	✗	0	<u>95.29</u>	<u>85.25</u> (+0.25)	<u>90.27</u> (+0.12)
Qwen2-VL 7B	✗	0	<u>96.47</u>	86.25	91.36
RC-Qwen2-VL 7B (Ours)	✗	0	97.06 (+0.59)	86.50 (+0.25)	<u>91.78</u> (+0.42)

TABLE IV: Experimental results (%) on personalized visual question answering. The best result in each setting is bold and the second is underlined. Weighted results are computed as arithmetic means.

questions to refer to an entity using information from one modality and ask about its information in another modality. Therefore, RC&P-Bench includes two types of questions: 1) 1738 visual-to-context questions. These questions refer to an entity based on its visual information in the image and asks about the content of its personalized information. 2) 1522 context-to-visual questions. These questions refer to an entity based on its personalized information and asks about its visual attributes in the image.

V. EXPERIMENTS

A. Training Details

We fine-tuned the Qwen2-VL-2B-Instruct and Qwen2-VL-7B-Instruct models using the LoRA method (rank = 8, alpha

	RCVQA			RCID		
	R	P	F1	R	P	F1
Proprietary						
Gemini Flash 1.5 8B	77.13	69.36	73.04	77.82	10.50	18.50
Gemini Flash 1.5	87.40	83.62	85.47	90.74	1.31	2.58
Gemini Flash 2.0	72.69	57.89	64.45	85.73	14.47	24.76
GPT-4o-mini	63.67	66.47	65.04	55.07	72.15	62.46
Open-source						
InternVL2-2B	1.24	55.93	2.44	4.17	62.73	7.82
InternVL2-4B	26.25	72.25	38.51	14.17	59.94	22.92
InternVL2-8B	60.13	80.23	68.74	24.92	47.95	32.80
MiniCPM V2.6 (8B)	74.20	74.67	74.43	51.32	49.44	<u>50.37</u>
Qwen2-VL-2B	15.31	0.22	0.43	44.78	18.55	26.24
RC-Qwen2-VL 2B (Ours)	<u>89.51</u> +74.20	<u>93.46</u> +93.24	<u>91.45</u> +91.02	<u>44.25</u> -0.53	<u>48.41</u> +29.86	<u>46.23</u> +19.99
Qwen2-VL-7B	61.15	66.58	63.75	30.81	21.81	25.54
RC-Qwen2-VL 7B (Ours)	92.57 +31.42	96.21 +29.63	94.35 +30.60	61.05 +30.24	53.82 +32.01	57.21 +31.67

TABLE V: Experimental results (%) of citation generation on the RCVQA and RCID tasks. Among open-source models, the best results are highlighted in **bold**, while the second-best results are underlined. RC-Qwen2-VL models lead their similarly sized open-source counterparts and outperform certain closed-source models.

= 16), while keeping the visual encoder frozen. Training was conducted for 20,000 steps with a batch size of 32 and a learning rate of $5.0e-5$, utilizing a cosine learning rate scheduler with a warmup ratio of 0.05. The training process was performed on 2 NVIDIA RTX 3090 GPUs in bfloat16 precision to optimize computational efficiency.

B. Experimental Results on RCMU Tasks

Settings. We evaluate the models' region-level context-aware multimodal (RCMU) capabilities on the RCMU test

set, comprising three tasks: Region-based Contextual Image Description (RCID), Region-based Contextual Visual Question Answering (RCVQA), and Multimodal Context-aware Content Generation (MCCG). We compare our models against state-of-the-art MLLMs, including proprietary models like Gemini Flash 1.5 8B [1], Gemini Flash 1.5 [1], Gemini Flash 2.0 [38], GPT-4o-mini [39] and open-source models such as InternVL2 series [40], [41], Qwen2-VL series [3]) and MiniCPM V2.6 [42]. For the RCID task, we employed RCIDScore to provide a comprehensive and fine-grained evaluation. The results from traditional metrics, such as BLEU [14], ROUGE-L [15], and CIDEr [16], are included in the appendix for reference. For the RCVQA task, we used the DeepSeek V3 [43] model to assess the correctness of the answers. For the MCCG task, following [44], we evaluated the recall, precision, and F1 score of citations. Specifically, citation recall refers to the percentage of sentences/responses that can be supported by the corresponding cited passages. Citation precision indicates the percentage of citations in the response that effectively support their respective sentences. The citation F1 score is the harmonic mean of citation recall and citation precision. We compute citation recall and citation precision following the approach outlined in [44], with one key difference: we consider images as a default source of information that does not require explicit citation. As a result, each sentence inherently has an implicit citation to the image, and we take this implicit citation into account during evaluation. We used Gemini Flash 1.5 [1] to determine whether a response is supported by the corresponding cited passages and images. The prompts used in the evaluation are displayed in the appendix.

a) Results on RCVQA and RCID: The results on RCVQA and RCID tasks are shown in Table II. For the RCVQA task, the RC-Qwen2-VL 2B and RC-Qwen2-VL 7B models significantly outperform all compared open-source and closed-source models, achieving an accuracy improvement of over 50% compared to the baseline Qwen-VL 2B and Qwen-VL 7B models. Notably, while most open-source models struggle with unanswered questions, RC-Qwen2-VL models demonstrate superior capability in addressing these challenges. For the RCID task, the RC-Qwen2-VL models achieved the highest RCIDScore, surpassing all the compared open-source and closed-source models, demonstrating exceptional capabilities in region-level context-aware image description generation. The descriptions generated by the RC-Qwen2-VL models showed significant improvements over the baseline models in terms of context coverage, accuracy, and consistency between textual and visual information. Furthermore, we observed that after RCVIT, the visual quality of descriptions generated by the RC-Qwen2-VL 7B model slightly declined. This may be attributed to the difficulty of balancing a comprehensive description of visual content with contextual relevance and fluency. In summary, the RC-Qwen2-VL models outperform both open-source and closed-source models in RCVQA and RCID, demonstrating strong RCMU capability.

b) Results on Multimodal Contextual Citation Generation: We assessed the quality of the citations generated by models in both the RCVQA and RCID tasks. Given the distinct nature of these tasks, RCVQA requires a citation to

		RC-Qwen2-VL 2B		RC-Qwen2-VL 7B	
Citation Annotation		wo/	w/	wo/	w/
RCVQA	V2C Acc	70.77	70.95	81.33	80.01
	C2V Acc	50.56	50.45	60.80	59.24
	UA V2C Acc	58.97	75.51	84.01	85.96
	UA C2V Acc	94.81	95.83	95.94	97.86
	Overall Acc	68.78	73.18	80.52	80.77
Citation in RCVQA	Recall	0	89.51	6.07	92.57
	Precision	NA	93.46	85.87	96.21
	F1 Score	NA	91.45	11.34	94.35
RCID	CC	94.44	97.38	95.67	97.98
	CA	93.95	97.09	95.46	95.17
	CVC	83.65	81.65	86.13	85.85
	Context Score	90.68	92.04	92.42	93.00
	LLM2Clip Score	70.05	68.67	77.28	73.92
	Final Score	79.04	78.66	84.18	82.37
Citation in RCID	Recall	9.90	44.25	14.84	61.05
	Precision	47.13	48.41	18.50	53.82
	F1 Score	16.37	46.23	16.47	57.21

TABLE VI: Ablation study on the impact of citation annotations in training data. Best results are highlighted in **bold**. UA stands for unanswerable.

P/N Ratio	V2C	C2V	UA V2C	UA C2V	Overall
wo/ UA data	69.63	50.45	1.95	0.11	30.54
1:1	67.45	47.33	68.74	94.59	69.53
2:1	68.43	46.99	63.56	92.11	67.77
4:1	69.07	48.22	54.34	87.03	64.67
1:2	65.98	43.10	70.42	95.72	68.80

TABLE VII: Ablation study on the impact of no-answer RCVQA data proportion in training on RCVQA performance. Models here were trained for 5000 steps. UA stands for unanswerable.

be appended at the end of the answer, while RCID involves providing citations at multiple relevant points throughout the description. The results are shown in Table V. In the RCVQA task, the RC-Qwen2-VL models demonstrate the highest citation quality among all open-source and closed-source models in the comparison, achieving top performance in citation recall, citation precision, and F1 score. When compared to the baseline models, the RC-Qwen2-VL models show significant improvements. For example, RC-Qwen2-VL 2B achieves an F1 score improvement of 91.02% compared to the baseline models, while RC-Qwen2-VL 7B demonstrates an improvement of 30.6%. In the RCID task, the RC-Qwen2-VL models achieve the highest citation recall and F1 score among open-source models, with the F1 score of RC-Qwen2-VL 7B matching the top performance of closed-source models. Compared to the baseline models, the RC-Qwen2-VL models demonstrate significant improvements, with the F1 score of RC-Qwen2-VL 2b rising by 19.99% and the F1 score of RC-Qwen2-VL 7b increasing by 31.67%. Overall, the RC-Qwen2-VL models excel in multimodal context citation generation tasks.

	Ref	τ
BLEU-1	✓	25.55
BLEU-4	✓	28.54
ROUGE-L	✓	29.71
METEOR	✓	47.42
CIDEr	✓	50.68
CLIPS	✗	0.19
RCIDS(ours)	✗	51.84

TABLE VIII: Correlations with human judgment.

Multimodal RAG



Introduce the person who is giving a speech in the picture.

Elon Reeve Musk is a businessman and U.S. special government employee, best known for his key roles in Tesla, Inc. and SpaceX, and his ownership of Twitter. Musk is the wealthiest individual in the world; as of February 2025, Forbes estimates his net worth to be US\$397 billion. A member of the wealthy South African Musk family, Musk was born in Pretoria before immigrating to Canada, acquiring its citizenship. ...

Caption the image.

Donald John Trump, the 47th president of the United States, stands next to Elon Reeve Musk, a businessman and U.S. special government employee, at a political rally.

Multimodal Personalized Understanding and Generation



Caption the image.

Jack, 20 years old, born in 1892 in Chippewa Falls, Wisconsin, USA, is hugging Rose, 17 years old, born in 1895 in Philadelphia, USA.

What is Rose wearing?

Rose is wearing a white dress with a pink sash.

From Titanic



Caption the image.

Frank, a salesman at Knox Manufacturing and resident of 115 Revolutionary Road, is sitting at a table with his wife April, a full-time housewife who once dreamed of being an actress. They are looking at each other.

From Revolutionary Road

Fig. 6: Showcase of our models in practical applications. Amazon Rekognition Service is used here for celebrity/personalized detection and recognition.

C. Experimental Results on Personalized Multimodal Understanding

Settings. We evaluate the model’s personalized multimodal understanding capabilities on RC&P-Bench and the personalized question answering benchmark introduced by Yo’LLaVA [34]. We follow the setup in the RAP [33] and employ a multimodal retriever. For these tasks, we use accuracy as the evaluation metric. We compare our models against state-of-the-art MLLMs, including proprietary models like Gemini Pro 2.5 [45], GPT-4o [39] and open-source models such as InternVL2 series [40], [41], Qwen2-VL series [3], MiniCPM V2.6 [42] and specialized personalized multimodal understanding models like MyVLM [35], Yo’LLaVA [34] and RAP [33]. We evaluated accuracy across three distinct settings. In the **Closed-World** setting, we assess the overall system’s accuracy, regardless of whether the correct information was retrieved. The **Open-World** setting, in contrast, considers ‘insufficient information’ a correct response when the necessary information is not retrieved. Finally, the **Oracle**

setting bypasses retrieval by directly providing gold evidence, thereby evaluating only the answer generation capability.

Results and Analysis. The results on RC&P-Bench are presented in Table III, showing that the RC-Qwen2-VL models achieve significant improvements over the baseline models. Specifically, RC-Qwen2-VL 2B shows a remarkable +23.43 boost in the Open-World Overall score and +13.10 in the Oracle setting compared to its Qwen2-VL 2B counterpart. The gains are even more pronounced for the larger model. RC-Qwen2-VL 7B surpasses its baseline by +17.95 in the Open-World Overall score and an impressive +21.93 in the Oracle setting. The most substantial individual improvements are seen in the Context-to-Visual (C2V) tasks, with RC-Qwen2-VL 7B gaining +38.25 in the Open-World C2V and +33.93 in the Oracle C2V tasks. Furthermore, the RC-Qwen2-VL 7B model has achieved state-of-the-art (SOTA) performance among open-source models and is comparable to or even surpasses top-tier proprietary models. For instance, in the Oracle setting, RC-Qwen2-VL 7B’s Overall score of 78.83% significantly outperforms other open-source models like InternVL2-8B (65.61%) and MiniCPM V2.6 (53.80%). Notably, this score also surpasses the proprietary GPT-4o (71.29%) and is highly competitive with Gemini Pro 2.5 (79.23%). This indicates that the capabilities of the RC-Qwen2-VL models, developed through region-level context-aware visual instruction tuning, can be effectively transferred to multimodal personalized understanding.

The results on the personalized question answering benchmark are presented in Table IV. Our proposed models demonstrate exceptional performance and efficiency. Specifically, the RC-Qwen2-VL 7B model sets a new state-of-the-art record on the visual personalized question answering task with a score of 97.06%. Critically, this is achieved in a zero-shot setting without requiring any extra personalized training, a stark contrast to other methods that depend on personalized tuning. Compared to its baseline, our method delivers consistent improvements across all metrics. The 7B model achieves a weighted average score of 91.78%, securing the second-highest rank among all methods and proving its strong competitiveness despite its smaller model size and more challenging setup.

D. Further Analyses

a) Ablation Study: We explored the effect of citation annotations in the training data on the region-level context-aware ability of the model. Specifically, we compared the model’s performance on training data with and without citation annotations. The experimental results are presented in Table VI. As shown, incorporating citation annotations into the training data significantly improves the quality of the generated citations and modestly enhances the model’s region-level context-aware multimodal understanding capability. However, this comes at the cost of reduced visual quality in the generated image descriptions.

We also investigated how varying the proportion of no-answer RCVQA data in the training set impacts the model’s RCVQA performance. Specifically, we trained five different RC-Qwen2-VL variants for 5000 steps each, under various

conditions: one with no no-answer RCVQA data, and others with different ratios of answerable to unanswerable RCVQA data (1:1, 2:1, 4:1, 1:2). The results are presented in Table VII. As shown, incorporating unanswerable RCVQA data into the training set significantly enhances the model’s performance on such questions. Furthermore, the model achieves its highest overall accuracy on the RCVQA task when the ratio of answerable to unanswerable RCVQA training data is 1:1.

To evaluate the consistency of image captioning metrics with human subjective judgment on Region-level context-aware image descriptions, we manually scored 500 (image, description) pairs. The scoring was based on a five-level scale: **Excellent**: No important visual or contextual information is missing; **Good**: Minor omissions of visual or contextual information; **Average**: Important visual or contextual information is missing; **Poor**: Either the visual or the contextual information is completely omitted; **Very Poor**: The caption is not acceptable due to grammatical errors, incomplete sentences, or other flaws. The experiment measures this consistency by calculating the Kendall’s Tau (τ) correlation coefficient between each metric’s scores and the human ratings. A higher correlation coefficient indicates that the results of the automatic evaluation metric align more closely with the standards of human judgment. The results are shown in Table VIII. The proposed reference-free metric, RCIDS, achieves the highest correlation score (51.84), demonstrating a stronger alignment with human assessment than all other tested metrics. Notably, it not only vastly outperforms the other reference-free metric, CLIPS (0.19), but also surpasses established reference-based standards like CIDEr (50.68), proving its state-of-the-art performance and utility in evaluating text quality without needing a ground truth reference.

VI. CONCLUSION

This paper introduces Region-level Context-aware Multimodal Understanding (RCMU), a new task requiring models to respond to instructions by integrating image content with textual information about specific regions or objects. The paper proposes Region-level Context-aware Visual Instruction Tuning (RCVIT) to equip MLLMs with this capability, along with the RCMU dataset for training and evaluation, and RCIDScore, a novel reference-free evaluation metric. Experiments show that models trained with RCVIT and the RCMU dataset outperform existing MLLMs on RCMU tasks and demonstrate applications in multimodal RAG and personalized conversation.

REFERENCES

[1] M. Reid, N. Savinov, D. Teplyashin, D. Lepikhin, T. P. Lillicrap, J.-B. Alayrac, R. Soricut, A. Lazaridou, O. Firat, J. Schrittwieser, I. Antonoglou, R. Anil, S. Borgeaud, A. M. Dai, K. Millican, E. Dyer, M. Glaese, T. Sottiaux, B. Jamin Lee, F. Viola, M. Reynolds, Y. Xu, J. Molloy, J. Chen, M. Isard, P. Barham, T. Hennigan, R. McLroy, M. Johnson, J. Schalkwyk, E. Collins, E. Rutherford, E. Moreira, K. W. Ayoub, M. Goel, C. Meyer, G. Thornton, Z. Yang, H. Michalewski, Z. Abbas, N. Schucher, A. Anand, R. Ives, J. Keeling, K. Lenc, S. Haykal, S. Shakeri, P. Shyam, A. Chowdhery, R. Ring, S. Spencer, E. Sezener, L. Vilnis, O. Chang, N. Morioka, G. Tucker, C. Zheng, O. Woodman, N. Attaluri, T. Kociský, E. Eltyshv, X. Chen, T. Chung, V. Selo, S. Brahma, P. Georgiev, A. Slone, Z. Zhu, J. Lottes, S. Qiao,

B. Caine, S. Riedel, A. Tomala, M. Chadwick, J. C. Love, P. Choy, S. Mittal, N. Houlsby, Y. Tang, M. Lamm, L. Bai, Q. Zhang, L. He, Y. Cheng, P. Humphreys, Y. Li, S. Brin, A. Cassirer, Y.-Q. Miao, L. Zilka, T. Tobin, K. Xu, L. Proleev, D. Sohn, A. Magni, L. A. Hendricks, I. Gao, S. Ontan’on, O. Bunyan, N. Byrd, A. Sharma, B. Zhang, M. Pinto, R. Sinha, H. Mehta, D. Jia, S. Caelles, A. Webson, A. Morris, B. Roelofs, Y. Ding, R. Strudel, X. Xiong, M. Ritter, M. Dehghani, R. Chaabouni, A. Karmarkar, G. Lai, F. Mentzer, B. Xu, Y. Li, Y. Zhang, T. L. Paine, A. Goldin, B. Neyshabur, K. Baumli, A. Levskaya, M. Laskin, W. Jia, J. W. Rae, K. Xiao, A. He, S. Giordano, L. Yagati, J.-B. Lespiau, P. Natsev, S. Ganapathy, F. Liu, D. Martins, N. Chen, Y. Xu, M. Barnes, R. May, A. Vezer, J. Oh, K. Franko, S. Bridgers, R. Zhao, B. Wu, B. Mustafa, S. Sechrist, E. Parisotto, T. S. Pillai, C. Larkin, C. Gu, C. Sorokin, M. Krikun, A. Guseynov, J. Landon, R. Datta, A. Pritzel, P. Thacker, F. Yang, K. Hui, A. Hauth, C.-K. Yeh, D. Barker, J. Mao-Jones, S. Austin, H. Sheahan, P. Schuh, J. Svensson, R. Jain, V. V. Ramasesh, A. Briukhov, D.-W. Chung, T. von Glehn, C. Butterfield, P. Jhakra, M. Wiethoff, J. Frye, J. Grimstad, B. Changpinyo, C. L. Lan, A. Bortsova, Y. Wu, P. Voigtlaender, T. N. Sainath, C. Smith, W. Hawkins, K. Cao, J. Besley, S. Srinivasan, M. Omernick, C. Gaffney, G. de Castro Surita, R. Burnell, B. Damoc, J. Ahn, A. Brock, M. Pajarskas, A. Petruskhina, S. Noury, L. Blanco, K. Swersky, A. Ahuja, T. Avrahami, V. Misra, R. de Liedekerke, M. Iinuma, A. Polozov, S. York, G. van den Driessche, P. Michel, J. Chiu, R. Blevins, Z. Gleicher, A. Recasens, A. Rustemi, E. Gribovskaya, A. Roy, W. Gworek, S. M. R. Arnold, L. Lee, J. Lee-Thorp, M. Maggioni, E. Piqueras, K. Badola, S. Vikram, L. Gonzalez, A. Baddepudi, E. Senter, J. Devlin, J. Qin, M. Azzam, M. Trebacz, M. Polacek, K. Krishnakumar, S. yiin Chang, M. Tung, I. Penchev, R. Joshi, K. Olszewska, C. Muir, M. Wirth, A. J. Hartman, J. Newlan, S. Kashem, V. Bolina, E. Dabir, J. R. van Amersfoort, Z. Ahmed, J. Cobon-Kerr, A. B. Kamath, A. M. Hrafnkelsson, L. Hou, I. Mackinnon, A. Frechette, E. Noland, X. Si, E. Taropa, D. Li, P. Crone, A. Gulati, S. Cevey, J. Adler, A. Ma, D. Silver, S. Tokumine, R. Powell, S. Lee, M. B. Chang, S. Hassan, D. Mincu, A. Yang, N. Levine, J. Brennan, M. Wang, S. Hodkinson, J. Zhao, J. Lipschultz, A. Pope, M. B. Chang, C. Li, L. E. Shafey, M. Paganini, S. Douglas, B. Bohnet, F. Pardo, S. Odoom, M. Rosca, C. N. dos Santos, K. Soparkar, A. Guez, T. Hudson, S. Hansen, C. Asawaroengchai, R. Addanki, T. Yu, W. Stokowiec, M. Khan, J. Gilmer, J. Lee, C. G. Bostock, K. Rong, J. Caton, P. Pejman, F. Pavetic, G. Brown, V. Sharma, M. Luvci’c, R. Samuel, J. Djolonga, A. Mandhane, L. L. Sjosund, E. Buchatskaya, E. White, N. Clay, J. Jiang, H. Lim, R. Hemsley, J. Labanowski, N. D. Cao, D. Steiner, S. H. Hashemi, J. Austin, A. Gergely, T. Blyth, J. Stanton, K. Shivakumar, A. Siddhant, A. Andreassen, C. L. Araya, N. Sethi, R. Shivanna, S. Hand, A. Bapna, A. Khodaei, A. Miech, G. Tanzer, A. Swing, S. Thakoor, Z. Pan, Z. Nado, S. Winkler, D. Yu, M. Saleh, L. Maggiore, I. Barr, M. Giang, T. Kagohara, I. Danilhelka, A. Marathe, V. Feinberg, M. Elhawaty, N. Ghelani, D. Horgan, H. Miller, L. Walker, R. Tanburn, M. Tariq, D. Shrivastava, F. Xia, C.-C. Chiu, Z. C. Ashwood, K. Baatarsukh, S. Samangoei, F. Alcober, A. Stjerngren, P. Komarek, K. Tshilas, A. Boral, R. Comanescu, J. Chen, R. Liu, D. Bloxwich, C. Chen, Y. Sun, F. aoyu Feng, M. Mauger, X. Dotiwalla, V. Hellendoorn, M. Sharan, I. Zheng, K. Haridasan, G. Barth-Maron, C. Swanson, D. Rogozi’nska, A. Andreev, P. K. Rubenstein, R. Sang, D. Hurt, G. Elsayed, R. shen Wang, D. Lacey, A. Ili’c, Y. Zhao, W. Han, L. Aroyo, C. Iwuanyanwu, V. Nikolaev, B. Lakshminarayanan, S. Jazayeri, R. L. Kaufman, M. Varadarajan, C. Tekur, D. Fritz, M. Khalman, D. Reitter, K. Dasgupta, S. Sarcar, T. Ornduff, J. Snaider, F. Huot, J. Jia, R. Kemp, N. Trdin, A. Vijayakumar, L. Kim, C. Angermueller, L. Lao, T. Liu, H. Zhang, D. Engel, S. Greene, A. White, J. Austin, L. Taylor, S. Ashraf, D. Liu, M. Georgaki, I. Cai, Y. Kulizhskaya, S. Goenka, B. Saeta, K. Vodrahalli, C. Frank, D. de Cesare, B. Robenek, H. Richardson, M. Alnahlawi, C. Yew, P. Ponnappalli, M. Tagliasacchi, A. Korchemniy, Y. Kim, D. Li, B. Rosgen, K. Levin, J. Wiesner, P. Banzal, P. Srinivasan, H. Yu, cCauglar Unlu, D. Reid, Z. Tung, D. F. Finkelstein, R. Kumar, A. Elisseeff, J. Huang, M. Zhang, R. Zhu, R. Aguilar, M. Gim’enez, J. Xia, O. Dousse, W. Gierke, S. H. Yeganeh, D. Yates, K. Jalan, L. Li, E. Latorre-Chimoto, D. D. Nguyen, K. Durden, P. Kallakuri, Y. Liu, M. Johnson, T. Tsai, A. Talbert, J. Liu, A. Neitz, C. Elkind, M. Selvi, M. Jasarevic, L. B. Soares, A. Cui, P. Wang, A. W. Wang, X. Ye, K. Kallarakal, L. Lohrer, H. Lam, J. Broder, D. N. Holtmann-Rice, N. Martin, B. Ramadhana, D. Toyama, M. Shukla, S. Basu, A. Mohan, N. Fernando, N. Fiedel, K. Paterson, H. Li, A. Garg, J. Park, D. Choi, D. Wu, S. Singh, Z. Zhang, A. Globerson, L. Yu, J. Carpenter, F. de Chaumont Quiry,

- C. Radebaugh, C.-C. Lin, A. Tudor, P. Shroff, D. Garmon, D. Du, N. Vats, H. Lu, S. Iqbal, A. Yakubovich, N. Tripuraneni, J. Manyika, H. Qureshi, N. Hua, C. Ngani, M. A. Raad, H. Forbes, A. Bulanova, J. Stanway, M. Sundararajan, V. Ungureanu, C. Bishop, Y. Li, B. Venkatraman, B. Li, C. Thornton, S. Scellato, N. Gupta, Y. Wang, I. Tenney, X. Wu, A. Shenoy, G. Carvajal, D. G. Wright, B. Bariach, Z. Xiao, P. Hawkins, S. Dalmia, C. Farabet, P. Valenzuela, Q. Yuan, C. A. Welty, A. Agarwal, M. Chen, W. Kim, B. Hulse, N. Dukkupati, A. Paszke, A. Bolt, E. Davoudi, K. Choo, J. Beattie, J. Prendki, H. Vashisht, R. Santamaria-Fernandez, L. C. Cobo, J. Wilkiewicz, D. Madras, A. Elqursh, G. Uy, K. Ramirez, M. Harvey, T. Liechty, H. Zen, J. Seibert, C. H. Hu, A. Y. Khorlin, M. Le, A. Aharoni, M. Li, L. Wang, S. Kumar, A. Lince, N. Casagrande, J. Hoover, D. E. Badawy, D. Soergel, D. Vnukov, M. Miecznikowski, J. Šimša, A. Koop, P. Kumar, T. Sellam, D. Vlasic, S. Daruki, N. Shabat, J. Zhang, G. Su, K. Krishna, J. Zhang, J. Liu, Y. Sun, E. Palmer, A. Ghaffarkhah, X. Xiong, V. Cotruta, M. Fink, L. Dixon, A. Sreevatsa, A. Goedeckemeyer, A. Dimitriev, M. Jafari, R. Crocker, N. Fitzgerald, A. Kumar, S. Ghemawat, I. Philips, F. Liu, Y. Liang, R. Sterneck, A. Repina, M. Wu, L. Knight, M. Georgiev, H. Lee, H. Askham, A. Chakladar, A. Louis, C. Crous, H. Cate, D. Petrova, M. Quinn, D. Owusu-Afriyie, A. Singhal, N. Wei, S. Kim, D. Vincent, M. Nasr, I. Shumailov, C. A. Choquette-Choo, R. Tojo, S. Lu, D. de Las Casas, Y. Cheng, T. Bolukbasi, K. Lee, S. Fatehi, R. Ananthanarayanan, M. Patel, C. E. Kaed, J. Li, J. Sygnowski, S. R. Belle, Z. Chen, J. Konzelmann, S. Poder, R. Garg, V. Koverkathu, A. Brown, C. Dyer, R. Liu, A. Nova, J. Xu, J. Bai, S. Petrov, D. Hassabis, K. Kavukcuoglu, J. Dean, O. Vinyals, and A. Chronopoulou, “Gemini 1.5: Unlocking multimodal understanding across millions of tokens of context,” *ArXiv*, vol. abs/2403.05530, 2024. [Online]. Available: <https://api.semanticscholar.org/CorpusID:268297180>
- [2] J.-B. Alayrac, J. Donahue, P. Luc, A. Miech, I. Barr, Y. Hasson, K. Lenc, A. Mensch, K. Millican, M. Reynolds, R. Ring, E. Rutherford, S. Cabi, T. Han, Z. Gong, S. Samangooei, M. Monteiro, J. Menick, S. Borgeaud, A. Brock, A. Nematzadeh, S. Sharifzadeh, M. Binkowski, R. Barreira, O. Vinyals, A. Zisserman, and K. Simonyan, “Flamingo: a visual language model for few-shot learning,” *ArXiv*, vol. abs/2204.14198, 2022. [Online]. Available: <https://api.semanticscholar.org/CorpusID:248476411>
- [3] P. Wang, S. Bai, S. Tan, S. Wang, Z. Fan, J. Bai, K.-Y. Chen, X. Liu, J. Wang, W. Ge, Y. Fan, K. Dang, M. Du, X. Ren, R. Men, D. Liu, C. Zhou, J. Zhou, and J. Lin, “Qwen2-vl: Enhancing vision-language model’s perception of the world at any resolution,” *ArXiv*, vol. abs/2409.12191, 2024. [Online]. Available: <https://api.semanticscholar.org/CorpusID:272704132>
- [4] Z. Chen, W. Wang, H. Tian, S. Ye, Z. Gao, E. Cui, W. Tong, K. Hu, J. Luo, Z. Ma, J. Ma, J. Wang, X. wen Dong, H. Yan, H. Guo, C. He, Z. Jin, C. Xu, B. Wang, X. Wei, W. Li, W. Zhang, B. Zhang, L. Lu, X. Zhu, T. Lu, D. Lin, and Y. Qiao, “How far are we to gpt-4v? closing the gap to commercial multimodal models with open-source suites,” *ArXiv*, vol. abs/2404.16821, 2024. [Online]. Available: <https://api.semanticscholar.org/CorpusID:269362546>
- [5] W. Dai, J. Li, D. Li, A. M. H. Tiong, J. Zhao, W. Wang, B. A. Li, P. Fung, and S. C. H. Hoi, “Instructblip: Towards general-purpose vision-language models with instruction tuning,” *ArXiv*, vol. abs/2305.06500, 2023. [Online]. Available: <https://api.semanticscholar.org/CorpusID:258615266>
- [6] H. Lu, W. Liu, B. Zhang, B.-L. Wang, K. Dong, B. L. B. Liu), J. Sun, T. Ren, Z. Li, H. Yang, Y. Sun, C. Deng, H. Xu, Z. Xie, and C. Ruan, “Deepseek-vl: Towards real-world vision-language understanding,” *ArXiv*, vol. abs/2403.05525, 2024. [Online]. Available: <https://api.semanticscholar.org/CorpusID:268297008>
- [7] W. Chen, H. Hu, X. Chen, P. Verga, and W. W. Cohen, “Murag: Multimodal retrieval-augmented generator for open question answering over images and text,” *ArXiv*, vol. abs/2210.02928, 2022. [Online]. Available: <https://api.semanticscholar.org/CorpusID:252735160>
- [8] H. Zhao, Z. Cai, S. Si, X. Ma, K. An, L. Chen, Z. Liu, S. Wang, W. Han, and B. Chang, “Mmicl: Empowering vision-language model with multimodal in-context learning,” *ArXiv*, vol. abs/2309.07915, 2023. [Online]. Available: <https://api.semanticscholar.org/CorpusID:261823391>
- [9] Y. Chen, S. Zhang, B. Han, T. He, and B. Li, “Camml: Context-aware multimodal learner for large models,” *ArXiv*, vol. abs/2401.03149, 2024. [Online]. Available: <https://api.semanticscholar.org/CorpusID:266844925>
- [10] B. A. Plummer, L. Wang, C. M. Cervantes, J. C. Caicedo, J. Hockenmaier, and S. Lazebnik, “Flickr30k entities: Collecting region-to-phrase correspondences for richer image-to-sentence models,” in *Proceedings of the IEEE international conference on computer vision*, 2015, pp. 2641–2649.
- [11] S. Kazemzadeh, V. Ordonez, M. Matten, and T. Berg, “Referitgame: Referring to objects in photographs of natural scenes,” in *Proceedings of the 2014 conference on empirical methods in natural language processing (EMNLP)*, 2014, pp. 787–798.
- [12] J. Yang, Y. Z. Ang, Z. Guo, K. Zhou, W. Zhang, and Z. Liu, “Panoptic scene graph generation,” in *European Conference on Computer Vision*. Springer, 2022, pp. 178–196.
- [13] H. Rasheed, M. Maaz, S. Shaji, A. Shaker, S. Khan, H. Cholakkal, R. M. Anwer, E. Xing, M.-H. Yang, and F. S. Khan, “Glamm: Pixel grounding large multimodal model,” in *Proceedings of the IEEE/CVF Conference on Computer Vision and Pattern Recognition*, 2024, pp. 13 009–13 018.
- [14] K. Papineni, S. Roukos, T. Ward, and W.-J. Zhu, “Bleu: a method for automatic evaluation of machine translation,” in *Proceedings of the 40th annual meeting of the Association for Computational Linguistics*, 2002, pp. 311–318.
- [15] C.-Y. Lin, “Rouge: A package for automatic evaluation of summaries,” in *Text summarization branches out*, 2004, pp. 74–81.
- [16] R. Vedantam, C. Lawrence Zitnick, and D. Parikh, “Cider: Consensus-based image description evaluation,” in *Proceedings of the IEEE conference on computer vision and pattern recognition*, 2015, pp. 4566–4575.
- [17] P. Anderson, B. Fernando, M. Johnson, and S. Gould, “Spice: Semantic propositional image caption evaluation,” in *Computer Vision—ECCV 2016: 14th European Conference, Amsterdam, The Netherlands, October 11–14, 2016, Proceedings, Part V 14*. Springer, 2016, pp. 382–398.
- [18] J. Li, D. Li, S. Savarese, and S. C. H. Hoi, “Blip-2: Bootstrapping language-image pre-training with frozen image encoders and large language models,” in *International Conference on Machine Learning*, 2023. [Online]. Available: <https://api.semanticscholar.org/CorpusID:256390509>
- [19] H. Liu, C. Li, Q. Wu, and Y. J. Lee, “Visual instruction tuning,” *ArXiv*, vol. abs/2304.08485, 2023. [Online]. Available: <https://api.semanticscholar.org/CorpusID:258179774>
- [20] H. Wei, L. Kong, J. Chen, L. Zhao, Z. Ge, J. Yang, J. Sun, C. Han, and X. Zhang, “Vary: Scaling up the vision vocabulary for large vision-language models,” *ArXiv*, vol. abs/2312.06109, 2023. [Online]. Available: <https://api.semanticscholar.org/CorpusID:266163175>
- [21] H. Zhang, H. You, P. Dufter, B. Zhang, C. Chen, H.-Y. Chen, T.-J. Fu, W. Y. Wang, S.-F. Chang, Z. Gan, and Y. Yang, “Ferret-v2: An improved baseline for referring and grounding with large language models,” *ArXiv*, vol. abs/2404.07973, 2024. [Online]. Available: <https://api.semanticscholar.org/CorpusID:269043094>
- [22] Y. Ma, Z. Wang, X. Sun, W. Lin, Q. Zhou, J. Ji, and R. Ji, “Inf-llava: Dual-perspective perception for high-resolution multimodal large language model,” *arXiv preprint arXiv:2407.16198*, 2024.
- [23] T. Chen, E. Zhang, Y. Gao, K. Li, X. Sun, Y. Zhang, H. Li, and R. Ji, “Mmicl: Boosting multi-modal fine-tuning with in-context examples,” *ACM Transactions on Multimedia Computing, Communications and Applications*.
- [24] P. Lu, S. Mishra, T. Xia, L. Qiu, K.-W. Chang, S.-C. Zhu, O. Tafjord, P. Clark, and A. Kalyan, “Learn to explain: Multimodal reasoning via thought chains for science question answering,” *Advances in Neural Information Processing Systems*, vol. 35, pp. 2507–2521, 2022.
- [25] T. Gao, P. Chen, M. Zhang, C. Fu, Y. Shen, Y. Zhang, S. Zhang, X. Zheng, X. Sun, L. Cao *et al.*, “Cantor: Inspiring multimodal chain-of-thought of mllm,” in *Proceedings of the 32nd ACM International Conference on Multimedia*, 2024, pp. 9096–9105.
- [26] B. Lin, B. Zhu, Y. Ye, M. Ning, P. Jin, and L. Yuan, “Video-llava: Learning united visual representation by alignment before projection,” in *Conference on Empirical Methods in Natural Language Processing*, 2023. [Online]. Available: <https://api.semanticscholar.org/CorpusID:265281544>
- [27] H. Zhang, X. Li, and L. Bing, “Video-llama: An instruction-tuned audio-visual language model for video understanding,” in *Conference on Empirical Methods in Natural Language Processing*, 2023. [Online]. Available: <https://api.semanticscholar.org/CorpusID:259075356>
- [28] Y. Luo, X. Zheng, X. Yang, G. Li, H. Lin, J. Huang, J. Ji, F. Chao, J. Luo, and R. Ji, “Video-rag: Visually-aligned retrieval-augmented long video comprehension,” *arXiv preprint arXiv:2411.13093*, 2024.
- [29] F. Li, R. Zhang, H. Zhang, Y. Zhang, B. Li, W. Li, Z. Ma, and C. Li, “Llava-next-interleave: Tackling multi-image, video, and 3d in large multimodal models,” *ArXiv*, vol. abs/2407.07895, 2024. [Online]. Available: <https://api.semanticscholar.org/CorpusID:271088459>
- [30] J. Ji, H. Wang, C. Wu, Y. Ma, X. Sun, and R. Ji, “Jm3d & jm3d-llm: Elevating 3d representation with joint multi-modal cues,” *IEEE Transactions on Pattern Analysis and Machine Intelligence*, 2024.

- [31] D. Driess, F. Xia, M. S. M. Sajjadi, C. Lynch, A. Chowdhery, B. Ichter, A. Wahid, J. Tompson, Q. H. Vuong, T. Yu, W. Huang, Y. Chebotar, P. Sermanet, D. Duckworth, S. Levine, V. Vanhoucke, K. Hausman, M. Toussaint, K. Greff, A. Zeng, I. Mordatch, and P. R. Florence, "Palm-e: An embodied multimodal language model," in *International Conference on Machine Learning*, 2023. [Online]. Available: <https://api.semanticscholar.org/CorpusID:257364842>
- [32] X. Li, M. Zhang, Y. Geng, H. Geng, Y. Long, Y. Shen, R. Zhang, J. Liu, and H. Dong, "Manipllm: Embodied multimodal large language model for object-centric robotic manipulation," *2024 IEEE/CVF Conference on Computer Vision and Pattern Recognition (CVPR)*, pp. 18 061–18 070, 2023. [Online]. Available: <https://api.semanticscholar.org/CorpusID:266573457>
- [33] H. Hao, J. Han, C. Li, Y.-F. Li, and X. Yue, "Rap: Retrieval-augmented personalization for multimodal large language models," in *Proceedings of the Computer Vision and Pattern Recognition Conference*, 2025, pp. 14 538–14 548.
- [34] T. Nguyen, H. Liu, Y. Li, M. Cai, U. Ojha, and Y. J. Lee, "Yo'llava: Your personalized language and vision assistant," *Advances in Neural Information Processing Systems*, vol. 37, pp. 40 913–40 951, 2024.
- [35] Y. Alaluf, E. Richardson, S. Tulyakov, K. Aberman, and D. Cohen-Or, "Myvlm: Personalizing vlms for user-specific queries," in *European Conference on Computer Vision*. Springer, 2024, pp. 73–91.
- [36] J. Hessel, A. Holtzman, M. Forbes, R. L. Bras, and Y. Choi, "Clipscore: A reference-free evaluation metric for image captioning," *arXiv preprint arXiv:2104.08718*, 2021.
- [37] W. Huang, A. Wu, Y. Yang, X. Luo, Y. Yang, L. Hu, Q. Dai, X. Dai, D. Chen, C. Luo *et al.*, "Llm2clip: Powerful language model unlock richer visual representation," *arXiv preprint arXiv:2411.04997*, 2024.
- [38] DeepMind, "Gemini 2.0: A new era of multimodal models," Google DeepMind Research Blog, 2024. [Online]. Available: <https://www.deepmind.com/blog/gemini-2-0-a-new-era-of-multimodal-models>
- [39] A. Hurst, A. Lerer, A. P. Goucher, A. Perelman, A. Ramesh, A. Clark, A. Ostrow, A. Welihinda, A. Hayes, A. Radford *et al.*, "Gpt-4o system card," *arXiv preprint arXiv:2410.21276*, 2024.
- [40] Z. Chen, W. Wang, H. Tian, S. Ye, Z. Gao, E. Cui, W. Tong, K. Hu, J. Luo, Z. Ma *et al.*, "How far are we to gpt-4v? closing the gap to commercial multimodal models with open-source suites," *arXiv preprint arXiv:2404.16821*, 2024.
- [41] Z. Chen, J. Wu, W. Wang, W. Su, G. Chen, S. Xing, Z. Muyan, Q. Zhang, X. Zhu, L. Lu, B. Li, P. Luo, T. Lu, Y. Qiao, and J. Dai, "Intern vl: Scaling up vision foundation models and aligning for generic visual-linguistic tasks," *2024 IEEE/CVF Conference on Computer Vision and Pattern Recognition (CVPR)*, pp. 24 185–24 198, 2023. [Online]. Available: <https://api.semanticscholar.org/CorpusID:266521410>
- [42] Y. Yao, T. Yu, A. Zhang, C. Wang, J. Cui, H. Zhu, T. Cai, H. Li, W. Zhao, Z. He *et al.*, "Minicpm-v: A gpt-4v level mllm on your phone," *arXiv preprint arXiv:2408.01800*, 2024.
- [43] A. Liu, B. Feng, B. Xue, B. Wang, B. Wu, C. Lu, C. Zhao, C. Deng, C. Zhang, C. Ruan *et al.*, "Deepseek-v3 technical report," *arXiv preprint arXiv:2412.19437*, 2024.
- [44] T. Gao, H. Yen, J. Yu, and D. Chen, "Enabling large language models to generate text with citations," *arXiv preprint arXiv:2305.14627*, 2023.
- [45] G. Comanici, E. Bieber, M. Schaeckermann, I. Pasupat, N. Sachdeva, I. Dhillon, M. Blistein, O. Ram, D. Zhang, E. Rosen *et al.*, "Gemini 2.5: Pushing the frontier with advanced reasoning, multimodality, long context, and next generation agentic capabilities," *arXiv preprint arXiv:2507.06261*, 2025.